Visualizing the Dynamics of EGFR Activity and Antiglioma Therapies *In vivo*

Esther Arwert, Shawn Hingtgen, Jose-Luiz Figueiredo, Henry Bergquist, Umar Mahmood, Ralph Weissleder, and Khalid Shah

Center for Molecular Imaging Research, Massachusetts General Hospital, Harvard Medical School, Boston, Massachusetts

Abstract

Many altered pathways in cancer cells depend on growth factor receptors. In primary malignant gliomas, the amplification/alteration of the epidermal growth factor receptor (EGFR) has been shown to play a significant role in enhancing glioma burden. In an effort to dissect the role of EGFR expression in glioma progression *in vivo* and evaluate targeted therapies for gliomas, we have genetically engineered glioma cells to visualize the dynamics of EGFR and targeted therapies in real time *in vivo*. Using engineered lentiviral vectors bearing fusions between EGFR and its exon 2 to 7 deleted variant (EGFRvIII) with green fluorescent protein (GFP) and *Renilla* luciferase (Rluc), we show that there is a direct correlation between EGFR expression and glioma cell proliferation in the initial stages of glioma progression. To monitor and evaluate EGFR-targeted therapies, we have engineered (*a*) short hairpin RNAs (shRNA) and (*b*) clinically used monoclonal antibody, cetuximab. Using EGFR-GFP-Rluc/firefly luciferase (Fluc)-DsRed2 glioma model, we show that both shRNAs and cetuximab result in a considerable reduction in glioma cell proliferation in culture and glioma burden *in vivo* that can be monitored in real time at a cellular resolution. This study serves as a template to follow the role of growth factor receptor expression in tumor progression and to image therapeutic efficacy of targeted therapies in cancer. [Cancer Res 2007;67(15):7335–42]

Introduction

Patients with glioblastoma multiforme (GBM) have median survival range of 9 to 12 months. In primary malignant gliomas, overexpression and amplification of epidermal growth factor receptor (EGFR) is found in 40% to 60% of the cases (1), making this the most frequent oncogenic change in GBMs. In GBMs, EGFR amplifications are often accompanied by gene rearrangements, resulting in seven known variants of EGFRs (2), of which the most common rearrangement is an in-frame deletion from exon 2 to 7, which results in a mutant receptor designated de2-7EGFR (EGFRvIII; ref. 3). Although EGFRvIII has a truncated extracellular domain and is incapable of binding EGF, the receptor is moderately but constitutively active (2–4) and has been shown to enhance the tumorigenic potential of glioma cells *in vivo* (4).

The fact that EGFR is frequently overexpressed and mutated in gliomas, thereby up-regulating different prosurvival pathways, makes it an excellent target for cancer therapy. Different approaches have been explored to target EGFR in GBMs, the most promising include the use of compounds such as gefinitib (Iressa, ZD1839) and erlotinib (Tarceva; OSI-774; ref. 5). These agents have been tested *in vitro* and in preclinical models and result in blocking the ligand-induced activation of the EGFR tyrosine kinase (6, 7). Other approaches include the use of monoclonal antibodies such as cetuximab (Erbitux, Mab-C225), panitumumab (ABX-EGF), and matuzumab (EMD72000), which block the binding of EGF to its receptor, prevent the activation of mitogen-activated protein kinase (MAPK), phosphatidylinositol 3-kinase/AKT (PI3K/AKT), signal transducers and activators of transcription (STAT), and phospholipase Cγ (PLCγ) signal transduction pathways (8), and result in G_1-phase cell cycle arrest and disruption of cell cycle progression (9). Recently, RNA interference (RNAi) to silence different variants of EGFR has been explored *in vivo* in glioma models (10–12). The lack of noninvasive assessment to monitor the intended target (EGFR expression) and the therapeutic efficacy of the newly developed therapies in real time in experimental glioma models is a major hindrance to further develop these specifically targeted and highly efficient therapies.

Noninvasive imaging based on quantitative and qualitative changes in light emission by fluorescent and bioluminescent markers [e.g., green fluorescent protein (GFP), DsRed2, firefly luciferase (Fluc), and *Renilla* luciferase (Rluc)] offers a huge potential to facilitate drug development. We have previously used fluorescence imaging to determine the transduction efficiency of engineered viruses on glioma cells (13, 14). In addition, we have also used dual bioluminescence imaging to follow the fate of neural stem cells and gliomas *in vivo* (15, 16). A combination of both fluorescent and bioluminescent marker in one transcript would facilitate the study of the expression of the intended target at different spatial resolution scales. Multiple approaches could be used to follow a molecular target or pathway with the fusion of a bioluminescent-fluorescent marker. For example, this reporter could be placed under the control of a transcriptional promoter that is responsive to the molecule or pathway of interest. In another approach, this reporter can be fused directly to the N or the C terminus of the mutated or overexpressed protein of interest.

In this study, we investigated whether engineered glioma cells with recombinant EGFRs could be used to simultaneously follow the EGFR expression and fate of gliomas *in vivo* in real time. Additionally, we investigated the effect of short hairpin RNAs (shRNA) targeting different variants of EGFR and clinically relevant monoclonal antibody–based glioma therapies in real time at a cellular resolution *in vivo*.

Materials and Methods

Generation of recombinant EGFR lentiviral vectors. The recombinant EGFR-GFP-Rluc plasmid constructs were constructed in CSCGW lentiviral

Note: Supplementary data for this article are available at Cancer Research Online (http://cancerres.aacrjournals.org/).

Requests for reprints: Khalid Shah, Center for Molecular Imaging Research, Massachusetts General Hospital, Harvard Medical School, Building 149, 13th Street, Charlestown, MA 02129. Phone: 617-726-4821; Fax: 617-724-5708; E-mail: kshah@helix.mgh.harvard.edu.

doi:10.1158/0008-5472.CAN-07-0077

vector (LV). LV-GFP-Rluc vector that bears a fusion of GFP and Rluc placed under a cytomegalovirus (CMV) promoter[1] was digested with *Nhe*1 and subjected to calf intestinal alkaline phosphatase (CIAP) treatment. Two fragments of EGFRvIII, an NH_2-terminal *Nhe*1/*Cla*1 2,080-bp fragment of EGFRvIII obtained from PLPc-EGFRvIII plasmid (kindly provided by Dr. Nabeel Bardeesy, Massachusetts General Hospital, Boston, MA) and a COOH-terminal 800-bp fragment obtained by PCR using a forward primer 5′-CCATCGATGTCTACATGATCATGG-3′ bearing a *Cla*I restriction site and a reverse primer 5′-CTAGCTAGCTGCTCCAATAAATTC-3′ bearing an *Nhe*1 site, were ligated into the *Nhe*1-digested LV-GFP-Rluc vector, resulting in a LV-EGFRvIII-GFP-Rluc construct. For constructing the LV-EGFR-GFP-Rluc construct, CSCGW vector was digested with *Nhe*1 and *Xho*I and the coding sequence for enhanced GFP was removed. A 2,500-bp *Cla*I/*Xho*I fragment (COOH-terminal fragment of EGFR + GFP-Rluc) obtained from LV-EGFRvIII-FP-Rluc construct and a 2,800-bp *Nhe*1/*Cla*I NH_2-terminal fragment of EGFR (obtained from PcB-EGFR) were ligated together into a *Nhe*1/*Xho*I-digested CSCGW vector. The construction of LV-GFP-Rluc and LV-Fluc-DsRed2 has been described previously.[1]

Generation of shRNA LVs. The shRNA plasmid constructs for EGFR and EGFRvIII were constructed in the pSuper vector (OligoEngine). The following oligonucleotides were used to generate double-stranded shRNAs: shEGFR-316 (starting on nucleotide 316 EGFR sequence), 5′-AGCTTCCC*CTCTGGAGGAAAAGAAAGTT*CTTCTGAAGAG*AACTTTCTTTTCCTCAAGAG*TTTTTTCTAGAC-3′ (forward) and 5′-CGTGTCTAGAAAAAA*CTCTGGAGGAAAAGAAAGTT*CTCTTCAGAAG*AACTTTCTTTTCCTCCAAGAG*GGGA-3′ (reverse); shEGFRvIII (over exon 1–8), 5′-AGCTTCCC*GAAAGGTAATTATGTGGTG*CTTCTGAAGAG*CACCACATAATTACCTTTC*TTTTTTCTAGAC-3′ (forward) and 5′-TCGTGTCTAGAAAAAA*GAAAGGTAATTATGTGGTG*CTCTTCAGAAG*CACCACAATTACCTTTC*GGGA-3′ (reverse). The annealed oligos were ligated in front of the polymerase III H1-RNA gene promoter in *Hin*dIII- and *Xho*I-digested pSUPER-neo-GFP. For generating small interfering RNA (siRNA) LVs, we amplified the inserts composed of the H1 promoter and the different siRNAs from the pSUPER-neo-GFP construct by PCR and cloned them into *Eco*RI/*Cla*I-digested pLVTHM LV (kindly provided by Dr. Dieder Trono, University of Geneva, Geneva, Switzerland). LVs were produced as described previously (17). In brief, the lentiviral genome (CMVR8.91) containing plasmid was transfected into 293T cells together with an envelope coding plasmid (VSVG) and vector constructs. LVs were harvested 40 h after transfection and concentrated by ultracentrifugation. Titers were determined on 293T cells as transducing units using serial dilutions of vector stocks with 8 mg/mL polybrene (Sigma). When necessary, drug selections of cells were done with 1 μg/mL puromycin or 10 μg/mL blasticidin after a 24-h recovery in standard growth medium.

Cell lines. Human glioma cell line, Gli36, and primary human glioma line, Gli79 (kindly provided by Dr. David Louis, Massachusetts General Hospital) and 293T cells were cultured in DMEM containing and supplemented with 10% fetal bovine, 100 μg/mL penicillin, and 100 μg/mL streptomycin. All cells were incubated at 37°C in a humidified 5% CO_2 incubator.

Cell sorting and flow cytometry. To generate glioma cells stably expressing recombinant EGFR fusions, Gli36 glioma cells were transduced with LV-EGFR-GFP-Rluc or LV-EGFRvIII-GFP-Rluc at a multiplicity of infection (MOI) of 1. Following expansion in culture, cells were sorted by fluorescence-activated cell sorting (FACSAria Cell-Sorting System, BD Biosciences). Two weeks after sorting, cells were analyzed by flow cytometry (FACSCalibur, BD Biosciences) to confirm that an equal number of cells were GFP positive in both cell lines.

Antibody labeling, EGF stimulation, and assays. For labeling EGFR monoclonal antibody, cetuximab (Imclone/Bristol-Myers Squibb) with a fluorescent dye, 15 mL cetuximab (2 mg/mL), was incubated overnight with 0.5 mg cy5.5 in 100 μL DMSO at 4°C. Subsequently, bound cy5.5 was separated from the free cy5.5 with a Sephadex G-25 column into PBS. The amount of attached dye was measured by direct absorbance at 680 nm, and the labeled antibody was quantified by bicinchoninic acid protein assay (Pierce Biotechnology). For determining the phosphorylation status of EGFR in Gli36 glioma cells expressing EGFR-GFP-Rluc, cells at 70% confluency were serum starved for 24 h and subsequently stimulated with 100 ng/mL EGF for 15 min. Cells were washed with PBS and lysed in radioimmunoprecipitation assay buffer. Fusion proteins were immunoprecipitated by incubating the cell lysate with 50 μL of anti–GFP-conjugated protein A-agarose beads (Roche Diagnostics) overnight at 4°C. Beads were washed and heated to 100°C for 5 min in the presence of protein loading buffer, and Western blotting was done as described below. For cetuximab-cy5.5 binding assays, Gli36-EGFR-GFP-Rluc cells were plated in a 96-well plate, serum starved for 24 h, and subsequently incubated in the medium bearing 8 ng/mL EGF and varying concentration of cetuximab-cy5.5 (0–100 μg/mL), and 90 min later, cells were washed and the amount of cell surface–bound cetuximab-cy5.5 was assessed by measuring the cy5.5 fluorescence at 650 nm. EC_{50} values were calculated using Prism (version 4.0a; GraphPad Software, Inc.). For luciferase assays, cells were seeded in different concentrations and, immediately before imaging, substrates for luciferases (1 μg/mL coelenterazine for Rluc and 1.5 μg/mL D-luciferin for Fluc) were added to the medium. Luciferase activity was measured using a cryogenically cooled high-efficiency CCD camera system (Roper Scientific). Each experiment was done thrice, with data points determined in triplicate.

LV-shRNA transduction and viability assays. Gli36 glioma cells or Gli79 primary glioma cells expressing Fluc-DsRed2 were transduced with LV-sh316 or LV-shvIII or control LV-shGFP at MOI of 3, and 1 week later, cells were harvested and subjected to immunoblotting with anti-GFP antibodies as described below. Number of viable Gli79 glioma cells 1 week after LV-sh316 and LV-shGFP transduction was assessed by luciferase-based viability assays (Promega).

SDS-PAGE and Western blotting. Cell samples were solubilized in protein loading buffer (33% glycerol, 6.6% SDS, 0.051 g/mL DTT), sonicated, boiled for ~10 min, and separated on 10% to 12% polyacrylamide gels. Proteins were transferred to a nitrocellulose membrane, blocked, and incubated with the following antibodies for 1 h: GFP (Invitrogen), EGFR (Stratagene), phosphorylated EGFR Tyr^{1068} (Cell Signaling), and tubulin clone DM1-A (Sigma-Aldrich). After washing, the membranes were incubated in horseradish peroxidase–labeled secondary antibodies for 1 h, washed, and detected using enhanced chemiluminescence agent (Pierce Biotechnology) according to the manufacturer's instructions. The autoradiographic film was scanned and subjected to quantification using the NIH Image program.[2]

Cell implantation, dual imaging, and intravital microscopy. Athymic nude mice (*nu/nu*; 6–7 weeks of age; Charles River Laboratories) were anesthetized by i.p. injection of a mix of ketamine (90 mg/kg) and xylazine (10 mg/kg) in saline. Four sets of experiments were done. (*a*) For correlation studies, mice ($n = 8$) were stereotactically implanted with varying number of (5×10^3 to 3×10^5) Gli36 glioblastoma cells expressing Fluc-DsRed2 and/or (vIII)EGFR-GFP-Rluc. Twenty-four hours after implantation, mice were imaged for Fluc expression. Specifically, mice were given i.p. injection of D-luciferin (4.5 mg/25 g body weight; prepared in 150 μL saline) and, 5 min later, imaged for Fluc activity for 1 min using a cryogenically cooled high-efficiency CCD camera system. (*b*) For studying EGFR expression and glioma proliferation simultaneously, mice ($n = 6$) were stereotactically implanted with 0.2×10^6 Gli36 glioblastoma cells expressing Fluc-DsRed2 and/or (vIII)EGFR-GFP-Rluc. Mice were sequentially imaged for 15 days after implantation for Fluc and Rluc expression. Fluc imaging was done as described above. For Rluc imaging, mice were given i.v. injection of coelenterazine (3.3 μg/g body weight) and imaged for Rluc activity for 5 min. Postprocessing and visualization were done as described previously (13). For intravital microscopy, a small circular portion of the cortical surface was exposed and the glioma cells were implanted stereotactically ($n = 6$) and imaging was done for a period of 15 days after glioma cell implantation, as described in the section below. (*c*) To image EGFR expression and cetuximab binding simultaneously, glioma cells expressing EGFR-GFP-Rluc were implanted as described above. Mice were imaged for the presence of gliomas by Rluc bioluminescence imaging. Mice bearing

[1] K. Shah, et al. Novel bimodal viral vectors and *in vivo* imaging reveal the fate of human neural stem cells in experimental glioma model, submitted for publication.

[2] http://rsb.info.nih.gov/nih-image/

gliomas (n = 6) were injected with cetuximab-cy5.5 (1 mg/mouse, tail vain injection) and intravital microscopy was done as described in the section below. (*d*) To follow the effect of cetuximab on Gli36-Fluc-DsRed2 glioma-bearing mice (n = 12), mice (n = 6) were treated with cetuximab (1 mg/mouse, tail vain injection) or saline (n = 6) every 2 days and imaged for Fluc activity as described above every 5 days for a period of 15 days. All animal protocols were approved by an institutional review board.

Intravital fluorescence microscopy. A prototype multichannel upright laser scanning fluorescence microscope (Olympus IV100) with a custom-designed stage and scanning unit for intravital observations was used for intravital microscopy (18). The stage was equipped with a heating plate regulated by a thermostat (37°C) and fluothane gas anesthesia. Mice were anesthetized as described above and placed on stereotactic apparatus to be imaged on confocal microscope. Images were acquired with FluoView imaging software (Olympus). Lasers used for excitation included a 488-nm argon laser, a 561-nm solid-state yellow laser, and a 633-nm HeNe-R laser. Emission signal was filtered using 505 to 525 nm, 586 to 615 nm, and 660 to 730 nm band-pass filters, respectively.

Histology on coronal brain sections and confocal fluorescent microscopy. After the last imaging round, mice were perfused by pumping ice-cold 4% paraformaldehyde directly into the heart for 5 min. The brains were removed and incubated in cold 4% paraformaldehyde for 4 to 6 h. Subsequently, the brains were placed in 15% sucrose for 8 to 12 h and 30% sucrose overnight before being embedded in OCT. Brain sections (10 μm) were subjected to fluorescent confocal microscopy.

Statistical analysis. Data are expressed as mean ± SD and were analyzed by either Student's t test or ANOVA (after Bartlett's test of homogeneity of variance) followed by the Newman-Keuls' correction for multiple comparisons. Differences were considered significant at $P < 0.05$.

Results

To study the role of EGFR and its variant, EGFRvIII, in glioma cell proliferation both *in vitro* and in animal models of glioma, we created fusions between two different variants of EGFR and a bioluminescent-fluorescent fusion protein marker, GFP-Rluc, and cloned them into LV plasmids. These plasmid constructs, diagrammed in Fig. 1*A*, were packaged into LV virions and used to transduce different glioma lines in culture. Fluorescent microscopy on human glioma cells transduced with LV-EGFR-GFP-Rluc or LV-EGFRvIII-GFP-Rluc or LV-GFP-Rluc revealed that most wild-type (wt) EGFR was expressed at the cell membrane and also seemed trapped inside cellular compartments (Fig. 1*B*). Flow cytometry showed equal numbers of GFP-positive cells following transduction with either LV-EGFR-GFP-Rluc or LV-EGFRvIII-GFP-Rluc (Fig. 1*C*). Immunoblotting with the anti-GFP antibody confirmed the expression of recombinant EGFR proteins (Fig. 1*D*). To confirm the functionality of the recombinant EGFR proteins, virally transduced human glioma cells were serum starved for 24 h and stimulated with 100 ng/mL EGF for 15 min before cells were harvested. Fusion proteins were immunoprecipitated, separated on SDS-PAGE, and immunoblotted with phosphorylated EGFR antibody specific for Tyr^{1068}. The phosphorylated proteins of correct size were seen in the lysates of both EGFR-GFP-Rluc–expressing and EGFRvIII-GFP-Rluc–expressing glioma cells (Fig. 1*E*). These results revealed that different variants of EGFR fused to marker proteins retain their characteristics and can be used to follow their expression both in culture and *in vivo*.

To monitor EGFR expression and glioma growth simultaneously in real time both *in vitro* and *in vivo*, we transduced EGFR-GFP-Rluc and EGFRvIII-GFP-Rluc Gli36 glioma cells with LV-Fluc-DsRed2 (Fig. 2*A* and *B*). Bioluminescence (Rluc) signal generated by cells expressing EGFR-GFP-Rluc and EGFRvIII-GFP-Rluc (Fig. 2*C* and *D*) in culture and *in vivo* (Fig. 2*E* and *F*) correlated linearly with cell number within the ranges tested, thus allowing quantification of EGFR expression in glioma cells. EGFR-GFP-Rluc/Fluc-DsRed2 and EGFRvIII-GFP-Rluc/Fluc-DsRed2 glioma cells were implanted into the right frontal lobe, and serial

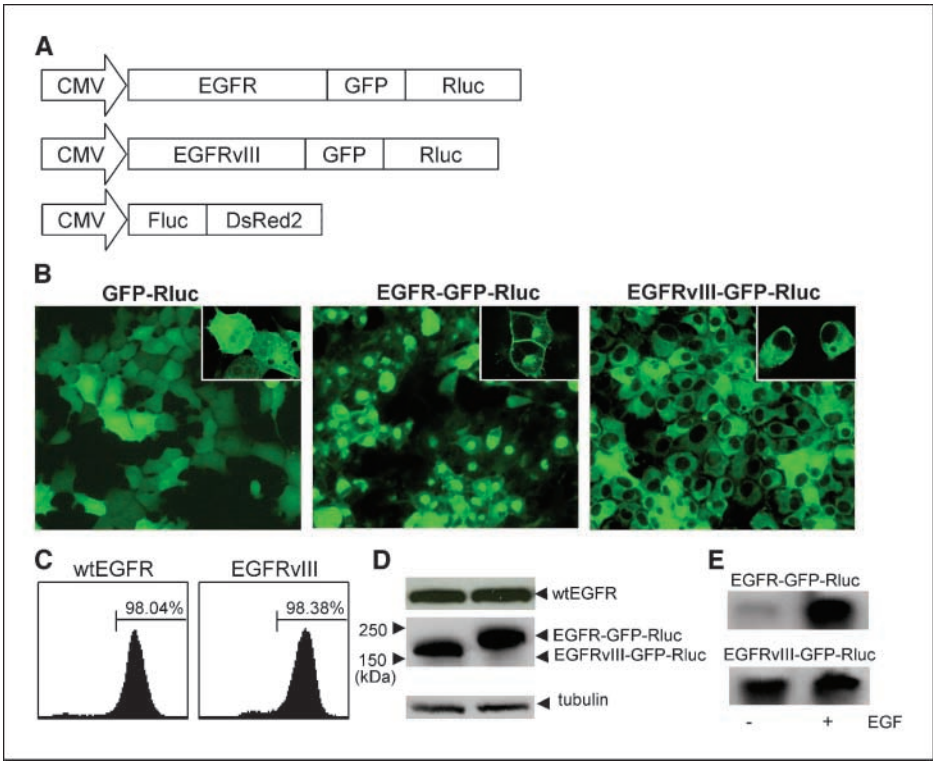

Figure 1. Transduced human glioma cells express functional recombinant EGFR proteins. *A,* a self-inactivating lentiviral system based on HIV-1 was used to construct vectors expressing fusions between EGFR and EGFRvIII with a fluorescent (GFP) and a bioluminescent (*Renilla* luciferase) fusion protein marker cloned in front of a CMV promoter and designated as LV-EGFR-GFP-Rluc and LV-EGFRvIII-GFP-Rluc. *B,* Gli36 human glioma cells were transduced with LV-EGFR-GFP-Rluc or LV-EGFRvIII-GFP-Rluc and visualized for GFP expression by confocal microscopy 24 h after transduction. Magnifications, ×20 and ×40 (insets). *C,* flow cytometry analysis of lentiviral-transduced Gli36 cells. *D,* immunoblot analysis to determine the levels of endogenous wtEGFR and recombinant EGFR in Gli36 cells transduced with LV-EGFR-GFP-Rluc or LV-EGFRvIII-GFP-Rluc. Tubulin was used as a loading control. *E,* transduced glioma cells were serum starved for 24 h and stimulated with EGF, harvested, immunoprecipitated, and immunoblotted with phosphorylated-specific EGFR antibody (Tyr^{1068}).

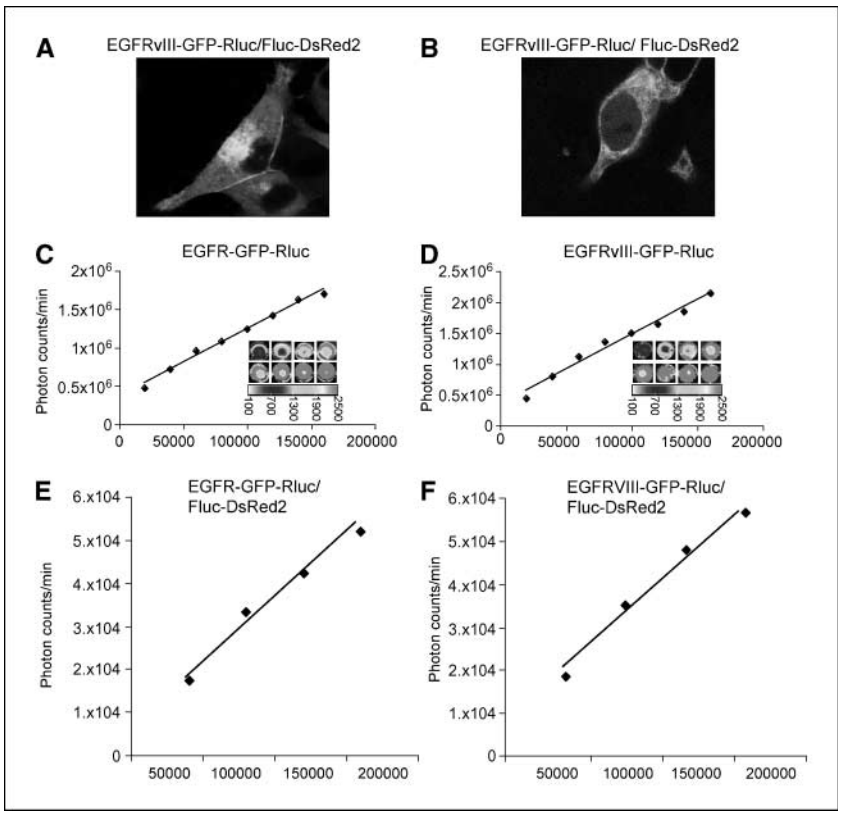

Figure 2. Expression and correlation of recombinant EGFR proteins *in vitro* and *in vivo*. Gli36 glioma cells, transduced with LV-EGFR-GFP-Rluc (*A*) or LV-EGFRvIII-GFP-Rluc (*B*) and cotransduced with LV-Fluc-DsRed2, were subjected to confocal fluorescence microscopy. Magnification, ×80. *C* and *D,* Gli36 glioma cells, expressing EGFR-GFP-Rluc (*C*) or EGFRvIII-GFP-Rluc (*D*), were plated in different concentrations and, 24 h later, incubated in a medium containing 1 μg/mL coelenterazine and imaged with a CCD camera is shown. Correlation between the number of cells and Rluc signal is shown. *E* and *F,* different concentrations of Gli36 glioma cells expressing EGFR-GFP-Rluc (*E*) or EGFRvIII-GFP-Rluc (*F*) and Fluc-DsRed2 were implanted into the frontal lobe of nude mice, and 24 h later, mice were imaged for Fluc expression by injecting mice with D-luciferin i.p. Correlation between the different number of implanted EGFR-GFP-Rluc/Fluc-DsRed2–expressing (*E*) and EGFRvIII-GFP-Rluc/Fluc-DsRed2–expressing (*F*) cells and the Fluc bioluminescent signal is shown.

Fluc and Rluc bioluminescence imaging was done on different days after implantation (Fig. 3*A* and *B*). The expression of both variants of EGFR was seen to increase overtime (Fig. 3*A*); however, EGFRvIII-expressing gliomas proliferated faster than the cells expressing the wt receptor (Fig. 3*A*). These findings are in line with the other studies that have shown that glioma cells expressing the vIII variant of EGFR proliferate more rapidly than the cells expressing the wt receptor (4). A direct correlation between the EGFR/EGFRvIII expression and glioma cell proliferation was observed until day 6 of glioma implantation; however, this correlation was seen to diminish between 6 and 10 days after glioma implantation (Fig. 3*C* and *D*). Intravital microscopy on mice bearing gliomas expressing EGFR-GFP-Rluc/Fluc-DsRed2 revealed the presence of GFP-positive receptors (Fig. 3*E*) in DsRed2-expressing single glioma cells *in vivo* (Fig. 3*F* and *G*). Furthermore, histology on coronal brain sections confirmed the presence of the GFP-expressing EGFR at the plasma membrane (Fig. 3*H*). These results reveal that different variants of EGFR and their influence on glioma proliferation can be followed in real time *in vivo*.

Next, we explored the possibility of monitoring EGFR-based antitumorigenic therapies using EGFR-GFP-Rluc and Fluc-DsRed2 expression in the glioma model. Two different approaches were explored. In the first approach, we used cetuximab, a clinically used monoclonal antibody that has been shown to block the EGF binding pocket of EGFR and results in G_1-phase cell cycle arrest and disruption of cell cycle progression (9). Cetuximab labeled with cy5.5 (cetuximab-cy5.5) was shown to bind EGFR-Rluc/Fluc-DsRed2 Gli36 cells with high affinity and had an EC_{50} value of 0.123 nmol/L (Supplementary Fig. S1*A*). Both cetuximab and cetuximab-cy5.5 were shown to inhibit glioma cell proliferation in culture at 50 μg/mL concentrations (Supplementary Fig. S1*B*). To simultaneously follow the binding of cetuximab-cy5.5 to the EGFR and the effect of cetuximab-cy5.5 on glioma proliferation *in vivo*, we injected cy5.5-labeled cetuximab (1 mg/mouse) i.v. into mice with established EGFR-Rluc/Fluc-DsRed2 Gli36 gliomas. Intravital microscopy done 48 h later revealed the binding of cetuximab-cy5.5 (blue) to EGFR-GFP/DsRed2–expressing glioma cells (Fig. 4*A*) with a very high specificity (Fig. 4*B*). Histology and confocal microscopy on coronal brain sections confirmed the binding of labeled cetuximab to the recombinant EGFR receptor (Fig. 4*C–E*). Mice bearing Fluc-DsRed2 Gli36 gliomas were injected with cetuximab (1 mg/mouse) every 3 days for a period of 15 days. Fluc bioluminescence imaging on cetuximab-treated mice revealed a considerable reduction in proliferation compared with the controls (Fig. 4*F*). These results reveal that the binding of cetuximab to recombinant EGFR can be followed in real time at a cellular resolution. Furthermore, administration of cetuximab i.v. into mouse with established gliomas results in considerable reduction in glioma volumes.

In the second approach, we developed shRNA-based targeted therapy to knock down different variants of EGFR. We designed two different shRNAs to specifically knock down EGFRvIII (shvIII) or both EGFR variants (sh316), and cloned them in front of the H1-RNA polymerase III promoter into LV plasmid that also bears GFP in front of the CMV promoter (Fig. 5*A*). Different glioma cells expressing EGFR-GFP-Rluc and EGFRvIII-GFP-Rluc were transduced with LVs bearing shRNAs (Fig. 5*B*). One week later, immunoblotting with anti-GFP antibody on proteins from harvested cells revealed that sh316 decreased both recombinant EGFR-GFP-Fluc and EGFRvIII-GFP-Rluc significantly (Fig. 5*C–F*), whereas shvIII decreased EGFRvIII in glioma cells (Fig. 5*D* and *F*).

To test the influence of blocking EGFR in glioma cells on their proliferation, we transduced Gli79 primary glioma line expressing Fluc-DsRed2 with LV-sh316 and followed the proliferation of cells over time. Fluc-based viability assays done 1 week later revealed a significant decrease in cell viability in LV-sh316–transduced cells compared with the controls (Fig. 5*G*). These results reveal that specific knockdown of different variants of EGFR can be achieved, which can be monitored in real time by following fluorescent protein expression marker. Furthermore, the knockdown of EGFR in primary glioma cells by sh316 results in the significant reduction in the cell proliferation, revealing the potential of shRNAs in developing antiglioma therapies.

Discussion

In this study, we have engineered recombinant EGFR and different therapeutic modalities to follow the dynamics of EGFR and antiglioma therapies *in vivo*. We show that there is a direct correlation between EGFR expression and glioma cell proliferation in the initial stages of glioma progression. Furthermore, cetuximab monoclonal antibody treatment and shRNA targeting EGFR result in a considerable reduction in glioma cell proliferation that can be followed in real time.

EGFR is one of the very important regulators of proliferation and cell survival pathways (19). In malignant gliomas, EGFR is frequently overexpressed and/or mutated into a constitutively

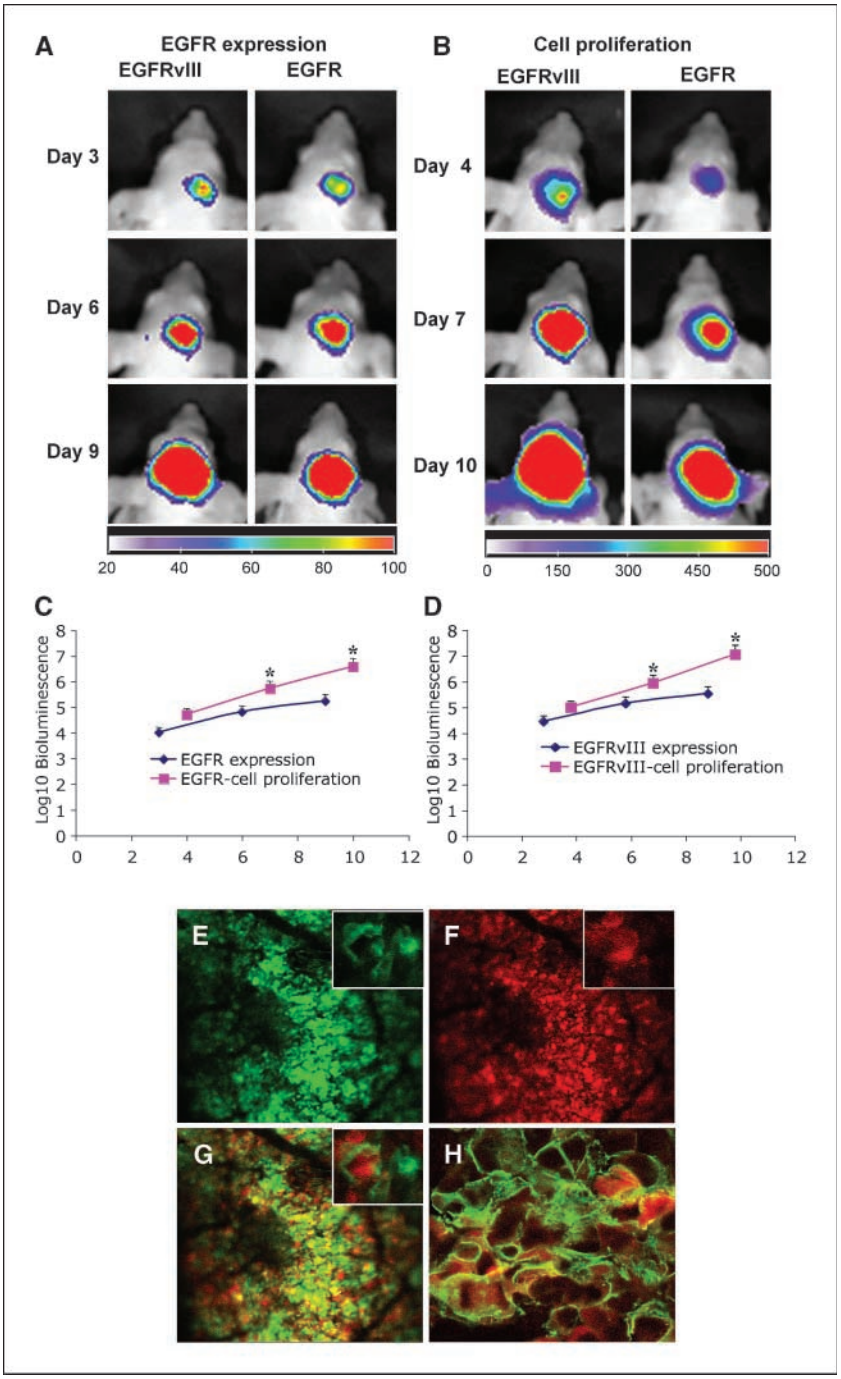

Figure 3. Real-time imaging of EGFR expression and glioma burden *in vivo*. Gli36 glioma cells expressing EGFR-GFP-Rluc or EGFRvIII-GFP-Rluc and Fluc-DsRed2 were implanted into the frontal lobe of nude mice, and mice were followed for 12 d by bioluminescence imaging. *A,* Rluc imaging: mice injected with coelenterazine via tail vain were imaged for EGFR expression by Rluc activity on days 3, 6, and 9 after glioma cell implantation. *B,* Fluc imaging: mice injected with D-luciferin i.p. and imaged for glioma proliferation by Fluc activity on days 4, 7, and 10 after glioma implantation. The images are a merge from the pseudocolor Rluc or Fluc activity image and the white light image of the mouse. The $\log_{10}$ bioluminescence intensities of wtEGFR-GFP-Rluc (*C*) and EGFRvIII-GFP-Rluc (*D*) expression and cell proliferation are plotted. *E* to *G,* mice with EGFR-GFP-Rluc/Fluc-DsRed2–expressing gliomas were imaged by intravital microscopy every 3 d for 15 d and sacrificed after the last imaging session. Intravital microscopy fluorescent images of day 6: EGFR-GFP-Rluc (*E*), Fluc-DsRed2 (*F*), and merge of (*E*), (*F*), and (*G*). Magnifications, ×8 and ×40 (insets). *H,* confocal images from histology on coronal brain sections showing the presence of EGFR-GFP-Rluc in the membrane of glioma cell. *Green,* EGFR-GFP-Rluc; *red,* Fluc-DsRed2. *Points,* mean; *bars,* SD. *, $P < 0.05$ versus EGFR expression.

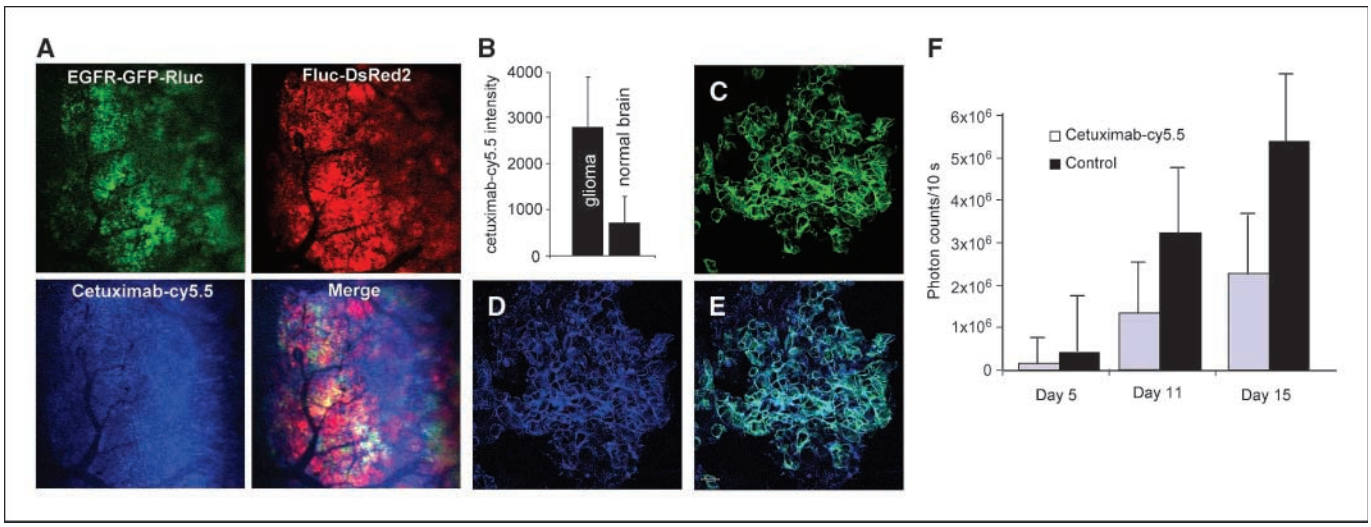

Figure 4. Monitoring monoclonal antibody–based therapies *in vivo*. Mice with established EGFR-GFP-Rluc–expressing and Fluc-DsRed2–expressing gliomas were injected with cetuximab-cy5.5 and, 3 d later, imaged by intravital microscopy. *A,* intravital fluorescent pictures of a day 4 EGFR-GFP-Rluc/Fluc-DsRed2 glioma: EGFR-GFP-Rluc (*green*), Fluc-DsRed2 (*red*), and cetuximab-cy5.5 (*blue*). *B,* cetuximab-cy5.5 binding to the normal brain cells compared with the glioma cells. *C* to *E,* confocal images from histology on coronal brain sections sacrificed on day 6 after implantation: EGFR-GFP-Rluc (*C*), cetuximab-cy5.5 (*D*), and merged image (*E*). *F,* mice with established Fluc-DsRed2–expressing gliomas were treated with cetuximab-cy5.5 every 3 d for a period of 2 wks and bioluminescence imaging was done to quantify the effects of cetuximab on glioma proliferation *in vivo*. *B, columns,* mean; *bars,* SD. *, $P < 0.05$ versus normal brain. *F, columns,* mean; *bars,* SD. *, $P < 0.05$ versus cetuximab-cy5.5.

active form, resulting in deregulation of growth and apoptosis (19). Because of its central role in glioma development, we engineered human glioma cells to express EGFR and EGFRvIII fused to GFP-Rluc to study the role of EGFR and EGFR-targeted therapies in the progression of gliomas. EGFR is a membrane protein and the recombinant EGFR proteins COOH-terminally fused to GFP and Rluc are therefore expected to be expressed at the plasma membrane. Whereas EGFRvIII-GFP-Rluc is specifically expressed at the cell surface, EGFR-GFP-Rluc is expressed both at the cell surface and also appears to be seen as "speckles" inside the human

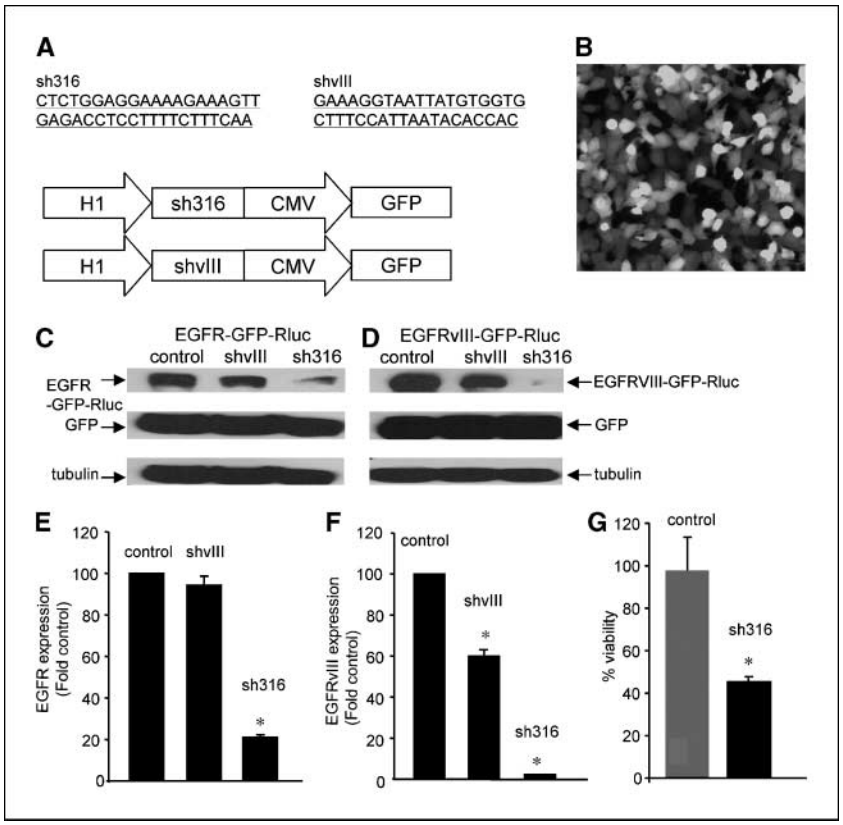

Figure 5. shRNAs against different variants of EGFR specifically target EGFR. *A,* shRNA sequences against wt and EGFRvIII were placed under an H1 promoter in an LV. *B,* transduction efficiency of LV-sh316 or LV-shvIII LVs on Gli36 human glioma as revealed by GFP fluorescence microscopy 36 h after transduction. Magnification, ×20. *C* to *F,* Gli36 cells expressing EGFR-GFP-Rluc (*C* and *E*) or EGFRvIII-GFP-Rluc (*D* and *F*) were transduced with shvIII and sh316, and after 1 wk, Western blotting was done with anti-GFP and anti-tubulin (loading control) antibodies. *Lanes 1* to *3,* protein samples from cells expressing EGFR-GFP-Rluc or EGFRvIII-GFP-Rluc with control shRNA (*lane 1*), shvIII (*lane 2*), or sh316 (*lane 3*). Protein bands were quantified using NIH Image. *E,* Gli79 cells, primary human glioma cells expressing Fluc-DsRed2, were transduced with sh316 or control shRNA, and 1 wk later, cell viability assays were done using luminescent ATP-based assay viability assays. *E* to *G, columns,* mean; *bars,* SD. *, $P < 0.05$ versus control.

glioma cells (Fig. 1*B*). This change in expression pattern might be due to the fact that wtEGFR is a large protein (170 kDa) compared with EGFRvIII (120 kDa), and therefore, the overexpressed EGFR-GFP-Rluc might be trapped in the endoplasmic reticulum. Furthermore, wtEGFR is internalized after EGF binding (20) and this might attribute to the fact that wtEGFR-GFP-Rluc is also seen in the cytoplasm as well as at the cell membrane.

Several studies have shown that EGFRvIII variant is more tumorigenic than the wtEGFR. Expression of EGFRvIII in fibroblast cells (21) or U87-MG glioma cells (4) resulted in increased growth of the tumor cells in a xenograft model. There is also evidence from transgenic mouse glioma models that EGFRvIII is more tumorigenic than the wt receptor (22, 23). Increased EGFRvIII expression may influence multiple aspects of tumor biology, including survival and/or proliferation of cells, motility, and invasiveness (24). To follow both EGFR variants *in vivo*, we used bioluminescent imaging that has been previously shown to be exceptionally useful for monitoring two molecular events in the same living animal (14, 16, 25). In our studies, we have shown that we can simultaneously follow both EGFR or EGFRvIII and glioma burden *in vivo* in real time. Gliomas expressing EGFRvIII-GFP-Rluc show higher proliferation than gliomas expressing wtEGFR-GFP-Rluc, indicating that we can monitor in real time the subtle differences in glioma cell proliferation and further confirming that gliomas expressing a constitutively active variant proliferate faster than the ones expressing the wtEGFR (4, 26). Furthermore, our studies indicate that glioma proliferation directly correlates with the receptor expression in the earlier stages of glioma growth but is slightly independent of the receptor expression in the later stages. There could be other factors such as heparin-binding EGF and transforming growth factor-α (27), which could influence the glioma growth in later stages.

The advantage of intravital microscopy over bioluminescence imaging is the ability to use florescent protein markers combined with high resolution in real time, thus evaluating the cellular and subcellular dynamics of EGFR. Our studies indicate that we can follow the receptor expression and glioma burden in live mice bearing glioma cells expressing EGFR-GFP-Rluc/Fluc-DsRed2. A recurrent challenge in developing tumor therapies is to non-invasively follow both the therapeutic drug as well as the target. Many studies have explored the effects of monoclonal antibody–based therapies specifically using cetuximab in GBMs (28–31). We labeled cetuximab with the fluorescent dye cy5.5 to follow the binding of antibody to the EGFR and to follow the effects of cetuximab on brain tumors in living mice. The advantage of cy5.5 over other fluorescent markers is that it has a different emission wavelength than GFP or DsRed2, thus making it possible to use it in our Gli36-Fluc-DsRed/EGFR-Rluc glioma cell model. Intravital fluorescent microscopy on nude mice bearing EGFR-GFP-Rluc/Fluc-DsRed2 gliomas revealed that cetuximab-cy5.5 colocalized with EGFR in glioma cells in living mice, suggesting that this approach may allow visualization of adequate dosing and kinetics of binding to glioma cells. Our results reveal that glioma cells expressing Fluc-DsRed2 and wtEGFR-GFP-Rluc or LV-EGFRvIII-GFP-Rluc can be used to test the efficacy of novel tumor therapies and study the effect of these novel approaches *in vivo*.

To test our glioma model system, we also explored the use of RNAi to target the EGFR. RNAi is selective and has both gene inhibition potency and relatively low toxicity (32). LVs were used for the delivery of the shRNAs into the cells because of their ability to transduce dividing as well as nondividing cells, their nontoxic nature, and their capacity to mediate stable long-term expression (33), which provided us the time to do the long-term experiments needed for RNAi. The strength of the knockdown was validated by monitoring GFP expression on Western blot, and our results showed that primary glioma cell proliferation was considerably decreased in the cells bearing shRNAs targeting EGFR. Although, RNAi offers a huge potential to specifically knock down the VIII variant of EGFR and holds promise as a preclinical and potentially as a clinical reagent, this mode of therapy is currently limited by delivery issues of gene- and cell-based therapies. The use of LV-mediated expression of shRNAs and noninvasive imaging methods should promote the use of RNAi as a preclinical reagent in mouse models of cancer.

Several biological pathways, including pathways relevant to cancer, are directly dependent on the action of cell membrane receptors. In principle, the approach described here should be generalizable to other growth factor receptors that are altered or overexpressed in a particular malignancy. Genetically engineered fusions of bioluminescent-fluorescent reporters and fluorescent tags for targets and drugs of pharmaceutical interest should expedite preclinical drug discovery.

Acknowledgments

Received 1/8/2007; revised 4/25/2007; accepted 5/25/2007.

Grant support: American Brain Tumor Association (K. Shah), Catherine and Pappas Award in Neuro-Oncology (K. Shah), NIH grant CAP5086355 (R. Weissleder), and National Cancer Institute grant CA86355 (R. Weissleder).

The costs of publication of this article were defrayed in part by the payment of page charges. This article must therefore be hereby marked *advertisement* in accordance with 18 U.S.C. Section 1734 solely to indicate this fact.

We thank Dr. David Louis for providing us with primary glioma lines, Vincent Lok for his help with coronal brain sections, and Fred Reynolds for labeling cetuximab with cy5.5 dye.

References

1. Watanabe K, Tachibana O, Sata K, et al. Overexpression of the EGF receptor and p53 mutations are mutually exclusive in the evolution of primary and secondary glioblastomas. Brain Pathol 1996;6:217–23; discussion 23–4.
2. Rasheed BK, Wiltshire RN, Bigner SH, et al. Molecular pathogenesis of malignant gliomas. Curr Opin Oncol 1999;11:162–7.
3. Wikstrand CJ, Reist CJ, Archer GE, et al. The class III variant of the epidermal growth factor receptor (EGFRvIII): characterization and utilization as an immunotherapeutic target. J Neurovirol 1998;4:148–58.
4. Nishikawa R, Ji XD, Harmon RC, et al. A mutant epidermal growth factor receptor common in human glioma confers enhanced tumorigenicity. Proc Natl Acad Sci U S A 1994;91:7727–31.
5. Halatsch ME, Schmidt U, Behnke-Mursch J, et al. Epidermal growth factor receptor inhibition for the treatment of glioblastoma multiforme and other malignant brain tumours. Cancer Treat Rev 2006;32:74–89.
6. Levitzki A, Gazit A. Tyrosine kinase inhibition: an approach to drug development. Science 1995;267:1782–8.
7. Sirotnak FM, Zakowski MF, Miller VA, et al. Efficacy of cytotoxic agents against human tumor xenografts is markedly enhanced by coadministration of ZD1839 (Iressa), an inhibitor of EGFR tyrosine kinase. Clin Cancer Res 2000;6:4885–92.
8. Adams GP, Weiner LM. Monoclonal antibody therapy of cancer. Nat Biotechnol 2005;23:1147–57.
9. Baselga J, Albanell J, Molina MA, et al. Mechanism of action of trastuzumab and scientific update. Semin Oncol 2001;28:4–11.
10. Liu XH, Yu EZ, Li YY, et al. RNA interference targeting Akt promotes apoptosis in hypoxia-exposed human neuroblastoma cells. Brain Res 2006;1070:24–30.
11. Saydam O, Glauser DL, Heid I, et al. Herpes simplex virus 1 amplicon vector-mediated siRNA targeting epidermal growth factor receptor inhibits growth of human glioma cells *in vivo*. Mol Ther 2005;12:803–12.
12. Zhang Y, Zhang YF, Bryant J, et al. Intravenous RNA interference gene therapy targeting the human epidermal growth factor receptor prolongs survival in intracranial brain cancer. Clin Cancer Res 2004;10:3667–77.
13. Shah K, Tang Y, Breakefield X, et al. Real-time

imaging of TRAIL-induced apoptosis of glioma tumors *in vivo*. Oncogene 2003;22:6865–72.
14. Shah K, Tung CH, Breakefield XO, et al. *In vivo* imaging of S-TRAIL-mediated tumor regression and apoptosis. Mol Ther 2005;11:926–31.
15. Tang Y, Shah K, Messerli SM, et al. *In vivo* tracking of neural progenitor cell migration to glioblastomas. Hum Gene Ther 2003;14:1247–54.
16. Shah K, Bureau E, Kim DE, et al. Glioma therapy and real-time imaging of neural precursor cell migration and tumor regression. Ann Neurol 2005;57:34–41.
17. Kock N, Kasmieh R, Weissleder R, et al. *In vivo* imaging of tumor therapy mediated by lentiviral expression of shBcl-2 and S-TRAIL. Neoplasia 2007;9:435–442.
18. Alencar H, Mahmood U, Kawano Y, et al. Novel multiwavelength microscopic scanner for mouse imaging. Neoplasia 2005;7:977–83.
19. Tagliaferri P, Tassone P, Blotta S, et al. Antitumor therapeutic strategies based on the targeting of epidermal growth factor-induced survival pathways. Curr Drug Targets 2005;6:289–300.
20. Orth JD, Krueger EW, Weller SG, et al. A novel endocytic mechanism of epidermal growth factor receptor sequestration and internalization. Cancer Res 2006;66:3603–10.
21. Batra SK, Castelino-Prabhu S, Wikstrand CJ, et al. Epidermal growth factor ligand-independent, unregulated, cell-transforming potential of a naturally occurring human mutant EGFRvIII gene. Cell Growth Differ 1995;6:1251–9.
22. Holland EC. Glioblastoma multiforme: the terminator. Proc Natl Acad Sci U S A 2000;97:6242–4.
23. Bachoo RM, Maher EA, Ligon KL, et al. Epidermal growth factor receptor and Ink4a/Arf: convergent mechanisms governing terminal differentiation and transformation along the neural stem cell to astrocyte axis. Cancer Cell 2002;1:269–77.
24. Boockvar JA, Kapitonov D, Kapoor G, et al. Constitutive EGFR signaling confers a motile phenotype to neural stem cells. Mol Cell Neurosci 2003;24:1116–30.
25. Bhaumik S, Walls Z, Puttaraju M, et al. Molecular imaging of gene expression in living subjects by spliceosome-mediated RNA trans-splicing. Proc Natl Acad Sci U S A 2004;101:8693–8.
26. Cavenee WK. Genetics and new approaches to cancer therapy. Carcinogenesis 2002;23:683–6.
27. Ramnarain DB, Park S, Lee DY, et al. Differential gene expression analysis reveals generation of an autocrine loop by a mutant epidermal growth factor receptor in glioma cells. Cancer Res 2006;66:867–74.
28. Barth RF, Wu G, Yang W, et al. Neutron capture therapy of epidermal growth factor (+) gliomas using boronated cetuximab (IMC-C225) as a delivery agent. Appl Radiat Isot 2004;61:899–903.
29. Eller JL, Longo SL, Hicklin DJ, et al. Activity of anti-epidermal growth factor receptor monoclonal antibody C225 against glioblastoma multiforme. Neurosurgery 2002;51:1005–13; discussion 1013–4.
30. Eller JL, Longo SL, Kyle M, et al. Anti-epidermal growth factor receptor monoclonal antibody cetuximab augments radiation effects in glioblastoma multiforme *in vitro* and *in vivo*. Neurosurgery 2005;56:155–62; discussion 162.
31. Wu G, Barth RF, Yang W, et al. Targeted delivery of methotrexate to epidermal growth factor receptor-positive brain tumors by means of cetuximab (IMC-C225) dendrimer bioconjugates. Mol Cancer Ther 2006; 5:52–9.
32. Fanning GC, Symonds G. Gene-expressed RNA as a therapeutic: issues to consider, using ribozymes and small hairpin RNA as specific examples. Handb Exp Pharmacol 2006;173:289–303.
33. Davidson BL, Breakefield XO. Viral vectors for gene delivery to the nervous system. Nat Rev Neurosci 2003;4: 353–64.

Visualizing the Dynamics of EGFR Activity and Antiglioma Therapies *In vivo*

Esther Arwert, Shawn Hingtgen, Jose-Luiz Figueiredo, et al.

Cancer Res 2007;67:7335-7342.